Autoantigens Targeted in Systemic Lupus Erythematosus Are Clustered in Two Populations of Surface Structures on Apoptotic Keratinocytes

By Livia A. Casciola-Rosen,* Grant Anhalt,* and Antony Rosen‡

*From the Departments of *Dermatology, and ‡Medicine, Johns Hopkins University School of Medicine, Baltimore, Maryland 21205*

Summary

Systemic lupus erythematosus is a multisystem autoimmune disease in which the autoantibody response targets a variety of autoantigens of diverse subcellular location. We show here that these autoantigens are clustered in two distinct populations of blebs at the surface of apoptotic cells. The population of smaller blebs contains fragmented endoplasmic reticulum (ER) and ribosomes, as well as the ribonucleoprotein, Ro. The larger blebs (apoptotic bodies) contain nucleosomal DNA, Ro, La, and the small nuclear ribonucleoproteins. These autoantigen clusters have in common their proximity to the ER and nuclear membranes, sites of increased generation of reactive oxygen species in apoptotic cells. Oxidative modification at these sites may be a mechanism that unites this diverse group of molecules together as autoantigens.

SLE is a multisystem autoimmune disease that is characterized by pleiotropy in its clinical and laboratory features (1). The autoantibody response in SLE is both diverse and exuberant, and targets a variety of nucleoprotein particles, some containing DNA (nucleosomes), and others RNA. The latter include small nuclear ribonucleoproteins (snRNPs),[1] cytoplasmic RNPs (SS-A/Ro), and ribosomes (2). Antibodies are also directed against negatively charged phospholipids (3). A striking feature of the different autoantigens in lupus is their lack of restriction to any one subcellular location: they may be exclusively nuclear, cytosolic, or membrane associated, or distributed between the nucleus and cytosol under different conditions. The proposal that the total repertoire of autoantigens might be clustered on a limited number of distinct subcellular particles is an attractive one (4), but such a cluster has not been identified to date.

The evolution of the autoantibody response to nucleosomes in lupus has been studied during clinical flares, as well as in animal models of the disease (5, 6). These studies have strongly indicated that the autoantibody response in lupus is antigen driven and T cell dependent. Thus, autoantibodies undergo isotype switching, somatic mutation, and affinity maturation that are characteristic of rechallenge of a primed immune system by antigen (for a review see reference 7). Furthermore, the presence of immune complexes containing double-stranded DNA (dsDNA) during acute flares (8) suggests that endogenous nucleosomes might be one of the antigens driving the immune response in this disease (5, 6).

A potential source of these antigenic components is the abundant generation of nucleosomes in cells undergoing apoptosis, as internucleosomal cleavage of DNA is a well-defined biochemical feature of this mode of cell death (9). The morphologic sequence of apoptosis has been well-defined, and follows an orderly process of nuclear condensation, surface blebbing, cytoplasmic contraction, and packaging of cellular components within membranes before their budding from the cell as apoptotic bodies (9). This reorganization is striking, as membrane, cytoplasmic, and nuclear components all appear at the surface of the dying cell. Apoptosis occurs in different cell types in a wide variety of organisms (9–12). It may occur in response to many different stimuli, including DNA damage (13, 14), growth factor deficiency (15), ligation of a family of cell surface receptors (16, 17), heat shock (18), and bacterial or viral infection (19, 20). Many of these stimuli generate reactive oxygen species, with consequent oxidative damage to multiple cellular targets (21). Furthermore, exposure to H_2O_2 (which generates ·OH radicals) also results in cell death with an apoptotic morphology, suggesting that oxidant stresses might function in a final common pathway leading to cell death (21). Bcl-2, a member of an interacting family of homologous proteins that modulate apoptosis (22, 23), has recently been shown to function in an antioxidant pathway that prevents apoptosis (21, 24).

The skin is a prominent target in patients with lupus, and the characteristic photosensitivity has been proposed to be a consequence of UV-driven autoantigen exposure with resultant antibody-dependent cellular cytotoxicity (25). Indeed, others have shown that UV irradiation of cultured monolayers

[1] *Abbreviations used in this paper:* dsDNA, double-stranded DNA; ER, endoplasmic reticulum; PI, propidium iodide; snRNP, small nuclear ribonucleoprotein; TMG, trimethylguanosine; TdT, terminal deoxynucleotidyl transferase.

 J. Exp. Med. © The Rockefeller University Press • 0022-1007/94/04/1317/14 $2.00
Volume 179 April 1994 1317–1330

of human keratinocytes changes the subcellular location of the ribonucleoprotein autoantigens Ro, La, Sm, and U1-RNP (26, 27). These antigens stained in a punctate pattern at the cell surface of irradiated cells, a site at which they were never present in unirradiated cells. Although UV irradiation induces apoptosis of keratinocytes (28), the correlation between altered autoantigen location and apoptosis has not previously been addressed.

In these studies, we have shown that autoantigens are clustered in two discrete populations of blebs at the surface of apoptotic cells. A population of small, abundant RNA-containing surface blebs stained intensely for Ro, and contained fragmented endoplasmic reticulum (ER) and ribosomes. The other population of larger blebs was less numerous and contained DNA (often nicked), surrounded by a rim of ribonucleoprotein antigens including Ro, La, and the snRNPs. These studies indicate that the clusters of autoantigens in lupus are confined to a cellular domain characterized by its proximity to ER and nuclear membranes. Study of these translocated autoantigen particles, and their ultimate fate, may provide a powerful system to explore the exposure and modification of autoantigens targeted in autoimmune disease.

Materials and Methods

Cell Culture and Irradiation. Human keratinocytes were obtained from neonatal foreskins, and cultured in Keratinocyte Growth Medium (KGM) (Clonetics Corp., San Diego, CA). All experiments were performed on confluent secondary monolayers. A panel of eight sunlamp bulbs (model FS40; Westinghouse, NJ) was used as a source of UVB. The UVB output, measured using a research radiometer (model Il 700; International Light Inc., Newburyport, MA) and a cosine corrected probe with a SCS 280 filter, was 0.5 mW/cm^2 at a distance of 19 cm. To perform irradiations, cells were washed twice with PBS (2.7 mM KCl, 1.5 mM KH_2PO_4, 137 mM NaCl, and 8 mM Na_2HPO_4) and irradiated in PBS. The cells were then incubated in KGM in a 5% CO_2 humidified incubator at 37°C. Initial dose–response and time course studies established that irradiation with 1,650 J/m^2 generated apoptotic cells within 6 h (data not shown). These conditions were used in all subsequent experiments.

DNA Extraction and Gels. DNA from whole cell populations was extracted, processed, and electrophoresed on 1.5% agarose gels as described (29).

Immunofluorescence and Confocal Microscopy. Immunofluorescence microscopy was performed on keratinocytes that were grown on No. 1 glass coverslips. Unless otherwise specified in the figure legends, cells were fixed with 4% paraformaldehyde (5 min, 4°C), before permeabilization with acetone (30 s, 4°C) and antibody staining. Ro, La, and U1-RNP were stained with human sera of defined specificities (diluted 1:160 in PBS) or affinity-purified antibodies, and were visualized with fluorescein-conjugated goat anti-human $F(ab')_2$ (Organon Teknika Corp./Cappel, Durham, NC). The 5′-trimethylguanosine (TMG) cap structures of snRNAs were labeled using a mouse mAb to TMG (Oncogene Science Inc., Uniondale, NY) according to the manufacturer's directions. Visualization was with biotinylated goat anti-mouse IgG (Southern Biotechnology Associates, Birmingham, AL) followed by BODIPY FL-2–conjugated streptavidin (Molecular Probes, Inc., Eugene, OR). BiP (GRP78) was stained using a mouse mAb (StressGen, Victoria, Canada), followed by incubation with biotinylated goat anti–mouse Ig (Southern Biotechnology Associates) and visualization with Texas red–conjugated streptavidin (Pierce, Rockford, IL). A mAb to ribosomal S1 was a generous gift from M. Schmidt-Zachmann (German Cancer Research Center, Heidelberg, FRG). α-mannopyranosyl and α-glucopyranosyl residues were stained with 0.1 mg/ml fluorescein-conjugated Con A (Molecular Probes, Inc.) either before or after permeabilization with acetone. Coverslips were mounted on glass slides with Permount® (Lipshaw, Pittsburgh, PA), before viewing and photography on a microscope (Axiophot; Carl Zeiss, Inc., Thornwood, NY) equipped with phase contrast and epifluorescence optics. Confocal microscopy was performed on a scanning confocal microscopy system (model MRC600; Bio-Rad Laboratories, Richmond, CA).

Nick Labeling of Apoptotic DNA. Nick labeling of apoptotic DNA in individual cells was performed as described (29), with the following modifications. Keratinocytes grown on coverslips were fixed with paraformaldehyde and acetone (see above) before incubation in terminal deoxynucleotidyl transferase (TdT) buffer. The endogenous peroxidase inactivation and proteinase K treatments were omitted. Horseradish peroxidase–coupled streptavidin (Southern Biotechnology Associates) was used at a 1:500 dilution before staining with 3-amino-9 ethyl carbazole (AEC) and visualization by light microscopy.

Electron Microscopy. Cells were grown on 35-mm tissue culture dishes, and irradiated according to standard procedures. 6 h after irradiation, monolayers were washed very gently with PBS, and fixed in 1% glutaraldehyde in 0.1 M sodium cacodylate, pH 7.4. Postfixation was in reduced osmium tetroxide. Monolayers were stained en-bloc with 1% uranyl acetate, before dehydration in ethanol, and embedding in Epon. Thin-sections were cut, and some were further stained with lead citrate before viewing and photography in an electron microscope (model TEM type 1A; Zeiss). Microwave fixation was performed as described (30), using a domestic microwave (General Electric, Louisville, KY) at full power for 20 s, such that a final fixative temperature of 50°C was obtained.

Enzyme Digests and Propidium Iodide Staining. Keratinocytes grown on coverslips were fixed, then incubated in a humidified container for 1 h at 37°C with 50 μg/ml heat-treated RNase (R-9009; Sigma Chemical Co., St. Louis, MO) or 140 U/ml RNase-free DNase (776785; Boehringer Mannheim, Indianapolis, IN). The enzyme stock solutions were diluted into buffer containing 25 mM Tris, pH 8, 5 mM $MgCl_2$, and 1 mM EDTA for the digests. Each experiment was controlled by performing identical incubations of cells in the presence of buffer only, or with both RNase and DNase. After enzyme digests, coverslips were washed in PBS before incubation with 5 μg/ml propidium iodide (PI) (30 s).

Antibody Screening Procedures. Reactivity of human autoimmune and control sera with saline soluble extracts of human spleen and rabbit thymus was determined by Ouchterlony double immunodiffusion using standard reference sera to Ro, La, Sm, and RNP (31).

Affinity Purification of Antibodies From Human Sera. Keratinocytes were lysed in Buffer A (1% NP-40, 20 mM Tris, pH 7.4, 150 mM NaCl, and 1 mM EDTA containing the following protease inhibitors: pepstatin A, leupeptin, antipain, chymostatin, and PMSF), and electrophoresed on 15% SDS-PAGE. 0.087% bisacrylamide was used to optimally separate the Ro and La proteins (32). The electrophoresed proteins were transferred to Immobilon® (Millipore Corp., Bedford, MA) (33) and used to affinity purify antibodies to 60-kD Ro, 48-kD La, and 70 kD U1-RNP proteins from human sera as described (34). The specificity of the affinity-purified anti-60-kD Ro was further confirmed by hemagglutination with a purified Ro–RBC conjugate (Hemagen, Waltham, MA). When we used the same procedure (34) to affinity purify antibodies to

52-kD Ro (three different sera were used in three separate attempts), we were unable to dissociate the bound antibodies from the Immobilon® with 0.2 M glycine, pH 2.8. Subsequent attempts to elute bound antibody with 3 M ammonium thiocyanate (35) resulted in a complete loss of antigen binding. We therefore used a patient serum that was monospecific for 52-kD Ro in immunoblotting and immunofluorescence (see Figs. 4 and 5, respectively).

Two-dimensional Gels and Western Blotting. Two-dimensional gel electrophoresis of keratinocyte lysates was performed as described (36), with the following modifications. After lysing the keratinocytes in Buffer A, the proteins were pelleted with TCA (36) and solubilized in buffer containing 9.5 M urea, 2% (vol/vol) ampholytes consisting of a mixture of 75% (pH 5–8), 25% (pH 3–10), 5% (vol/vol) 2-ME and 2% (vol/vol) NP-40. The isoelectric focusing gels consisted of 4% acrylamide, 9.5 M urea, and 2% (vol/vol) ampholytes made with the same proportions as above. Electrophoresis in the second dimension was performed on 15% SDS-polyacrylamide gels with 0.087% bis (32), and the proteins were then transferred to Immobilon® (33). Immunoblotting was performing using enhanced chemiluminescence according to the manufacturer's directions (Amersham, Arlington Heights, IL).

Results

UV Irradiation Induces Apoptosis in Keratinocytes. Keratinocyte monolayers were irradiated with UVB in order to induce apoptotic cell death. Within 6 h of irradiation, the asynchronous onset of apoptosis was detectable by phase contrast microscopy. Apoptotic cells were rounded up, pulled apart from their neighbors, and showed prominent surface blebbing (Fig. 1 *B* [37]). Apoptosis was confirmed by detection of internucleosomal cleavage of DNA in irradiated populations (Fig. 1 *A*, lane *2*), in contrast to the DNA from unirradiated populations which remained intact (Fig. 1 *A*, lane *1*). The correlation of morphologic changes with multiple internucleosomal nicks was assessed by introducing biotinylated dUTP at nicked sites with TdT (29). The labeled chromatin appeared condensed, and was found in morphologically apoptotic cells. In cells where the nucleus had already fragmented, the multiple apoptotic bodies formed were also strongly labeled (Fig. 1 *B*). No labeling was obtained in irradiated cells when TdT was omitted, and labeled cells were extremely rare in unirradiated keratinocytes (data not shown). Electron microscopy of irradiated cells demonstrated condensation of chromatin and fragmentation of the nucleus (Fig. 1 *C*). Cytoplasmic contraction was accompanied by fragmentation of intracellular membranes, whereas mitochondria appeared normal. These ultrastructural features are consistent with the morphology of apoptosis (9).

Small Surface Blebs on Apoptotic Keratinocytes Contain RNA. In our initial studies, we visualized chromatin condensation in apoptotic cells with PI staining after RNase digestion. When RNase treatment was serendipitously omitted, we noted that the small surface blebs on apoptotic cells were intensely labeled by PI, indicating that they contained RNA. To define the nucleic acid contents of the small apoptotic blebs more precisely, we examined their sensitivity to various nuclease digestions. In the absence of nuclease treatment, surface blebs stained strongly with PI, whereas the cytoplasm stained only weakly. Nuclear staining was prominent, with

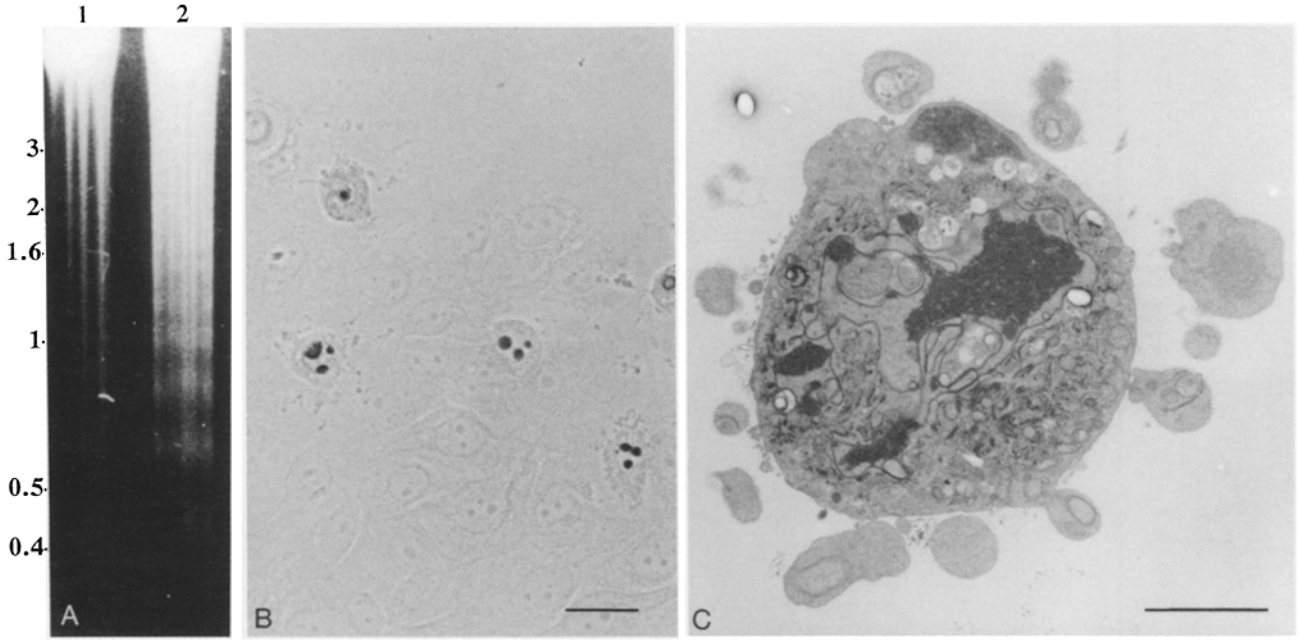

Figure 1. UVB irradiation of keratinocytes induces apoptosis. (*A*) Agarose gel electrophoresis of DNA obtained from irradiated (lane *2*) or unirradiated (lane *1*) keratinocytes. The migration positions of marker DNA are indicated in kilobase pairs on the left. The characteristic ladder pattern of fragmented DNA is seen in lane *2*. (*B*) Irradiated keratinocytes were nick endlabeled. Nicked DNA is visualized as the dark AEC reaction product. (*C*) Irradiated keratinocytes were fixed in glutaraldehyde and processed for electron microscopy. Cytoplasmic contraction, condensation of chromatin, and fragmentation of the nucleus are evident, whereas mitochondria appear normal. The data shown are representative of those obtained in two (*C*) or four (*A* and *B*) experiments. Bars: (*B*) 15 μm; (*C*) 3 μm.

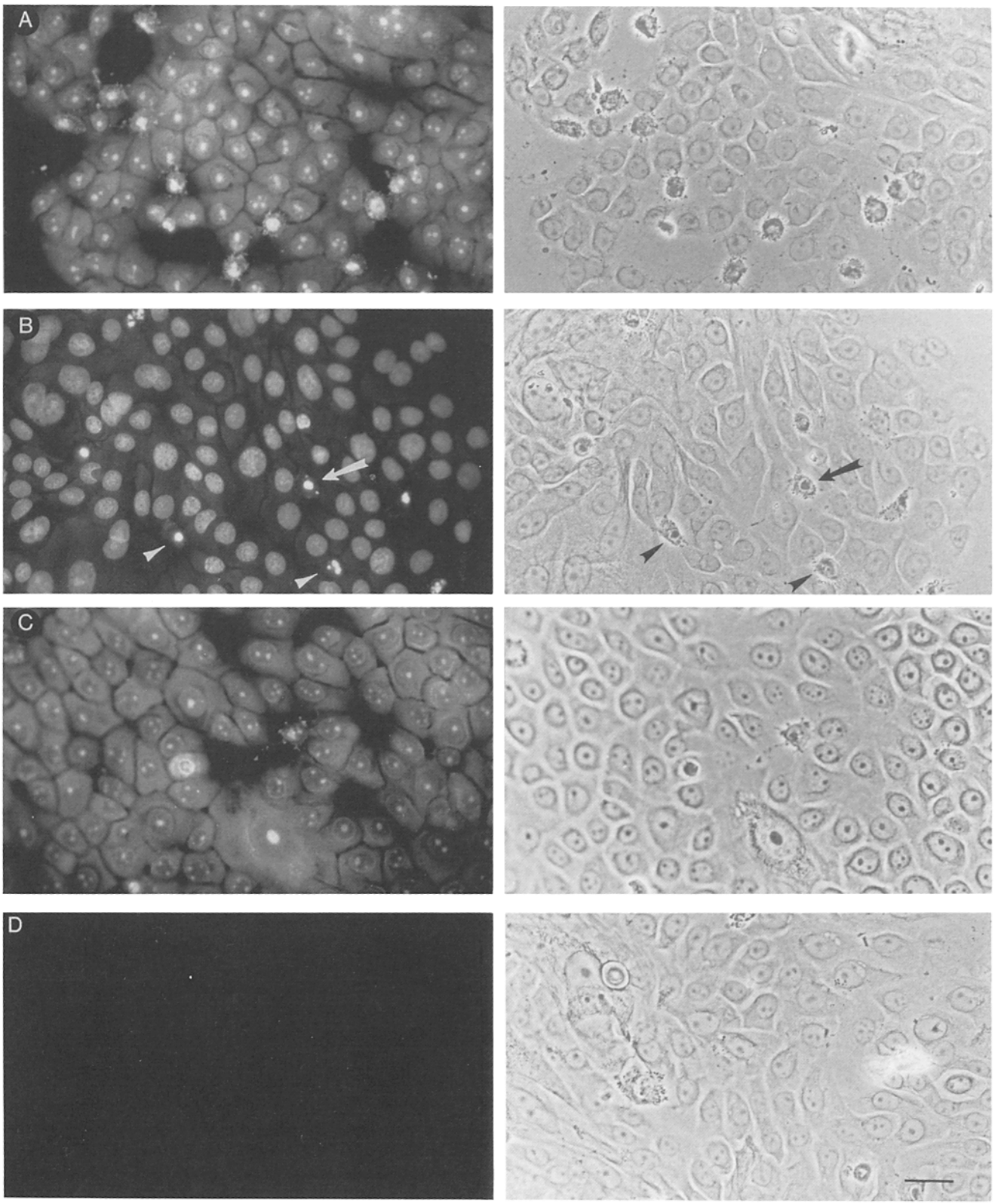

Figure 2. PI staining of nuclease-digested keratinocytes. Irradiated keratinocytes were treated with RNase (*B*), DNase (*C*), RNase plus DNase (*D*), or no enzymes (*A*). The cells were then stained with PI and viewed by immunofluorescence microscopy. (*Left*) Corresponding immunofluorescence and (*right*) phase pictures are shown. The nucleic acid contents of small surface blebs are sensitive to RNase, but not DNase. The data shown are representative of those obtained in four separate experiments. Bar, 20 μm.

conspicuous nucleoli (Fig. 2 *A*). In contrast, unirradiated keratinocytes showed diffuse cytoplasmic staining, as well as prominent nuclear and nucleolar staining (see Fig. 5 *E*). When irradiated cells were pretreated with RNase, the small surface blebs remained clearly visible by phase contrast microscopy, but were no longer stained with PI (Fig. 2 *B*, *arrowheads*). Condensed nuclear chromatin was obvious in these blebbed cells, and often showed the breaking up of the nucleus into several discrete fragments. Occasionally, these condensed nuclear fragments were seen at the cell surface in larger blebs (Fig. 2 *B*, *arrows*). These larger blebs also stained with the DNA-specific stain, 4',6-diamidino-2-phenylindole, dihydrochloride (DAPI) (data not shown), and could be nick labeled in the TdT assay (Fig. 1 *B*). Pretreatment with DNase did not affect the staining of small surface blebs, which stained strongly with PI under these conditions (Fig. 2 *C*). In these cells, the nuclear matrix staining had completely disappeared, making the nucleoli even more prominent. No PI staining was seen when irradiated cells were pretreated with both DNase and RNase (Fig. 2 *D*).

We further defined the RNA-containing surface blebs with confocal microscopy. Accumulation of PI was only visible at the cell surface, and we were never able to visualize similar aggregates of PI within the cytosol (Fig. 3 *A*). Indeed, cytosolic PI staining in apoptotic cells was diminished when compared with nonapoptotic cells (see and compare Fig. 5, *B* and *E*). Furthermore, Z-series and vertical sectioning showed that the blebs were restricted to the apical surface (Fig. 3 *B*). The small surface blebs were 1.3 ± 0.3 μm (mean ± SD, n = 54) in size, and were a common feature in apoptotic cells (both polarized and nonpolarized), including human fibroblasts, A431 cells, and Hep2 cells (data not shown). Blebs were always restricted to the nonadherent cell surface, and were present regardless of the initiating stimulus for apoptosis, which included irradiation, heat shock, or incubation in H_2O_2 (data not shown). Blebs were numerous in apoptotic keratinocytes with an intact, condensed nucleus, and were more prominent in these cells than in those where nuclear fragmentation was advanced. PI staining was heterogeneous in different blebs: some stained strongly and diffusely with PI, others appeared speckled, and still others contained small central areas that did not stain with PI. These RNA-containing surface blebs could readily be distinguished from apoptotic bodies since the latter (*a*) tended to be larger (mean diameter 2.7 ± 0.7 μm), (*b*) were fewer in number (3–10/cell), (*c*) contained DNA, (*d*) were present when nuclear fragmentation was advanced, and (*e*) were detected within the cytoplasm as well as in surface blebs. Both populations of surface blebs could be seen undergoing phagocytosis by surrounding nonapoptotic keratinocytes (data not shown).

Ribonucleoprotein Autoantigens Redistribute in Apoptotic Cells. We used antibodies to the ribonucleoprotein autoantigens

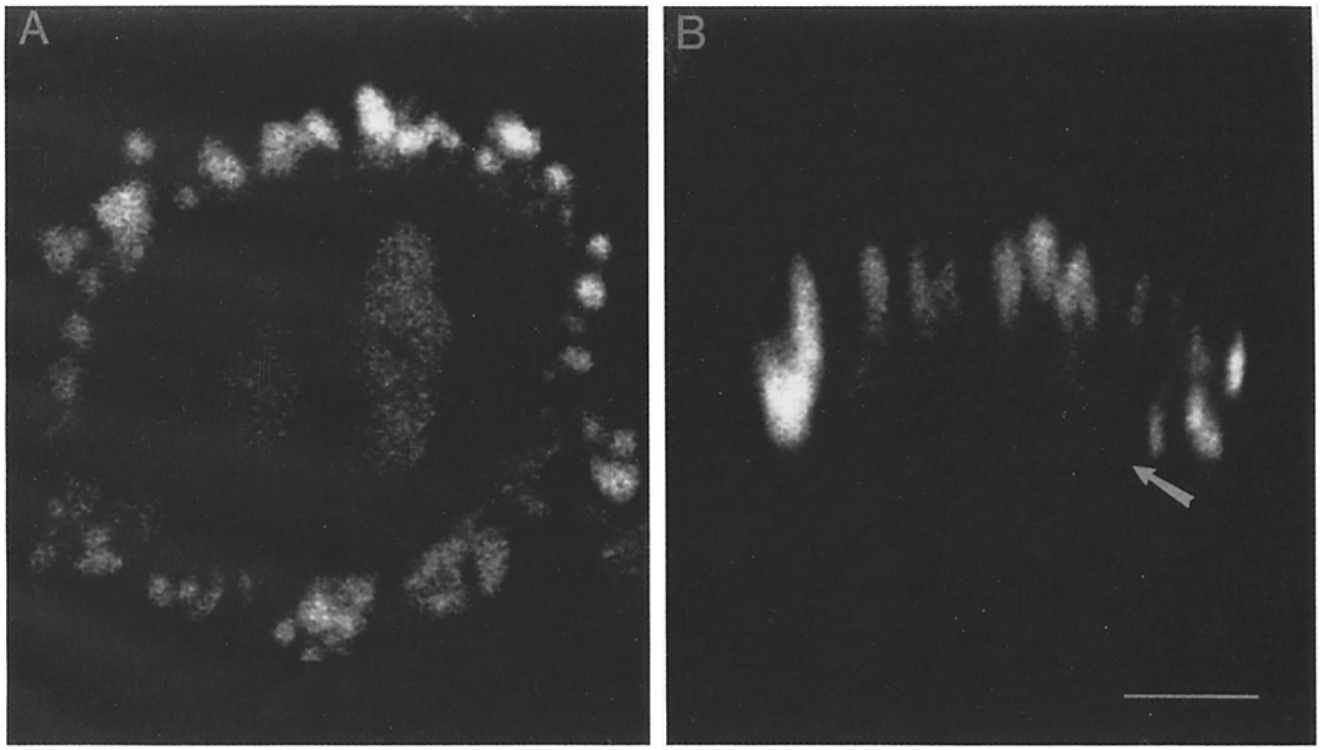

Figure 3. PI-stained blebs are only detected at the surface of irradiated keratinocytes. Irradiated keratinocytes were stained with PI and visualized with confocal microscopy. (*A*) Horizontal optical section through the upper surface of an apoptotic keratinocyte (the picture shown is one obtained in a Z-series). Note that the optical section includes only the uppermost tip of the nucleus, which is visible as the fainter PI staining in the central area of the cell. Surface blebs stain strongly with PI. (*B*) Vertical section through the same apoptotic keratinocyte shown in (*A*). The PI-stained blebs are restricted to the apical surface. (*Arrow*) Position of the coverslip. The data shown are representative of those obtained in eight different experiments. Bar, 10 μm.

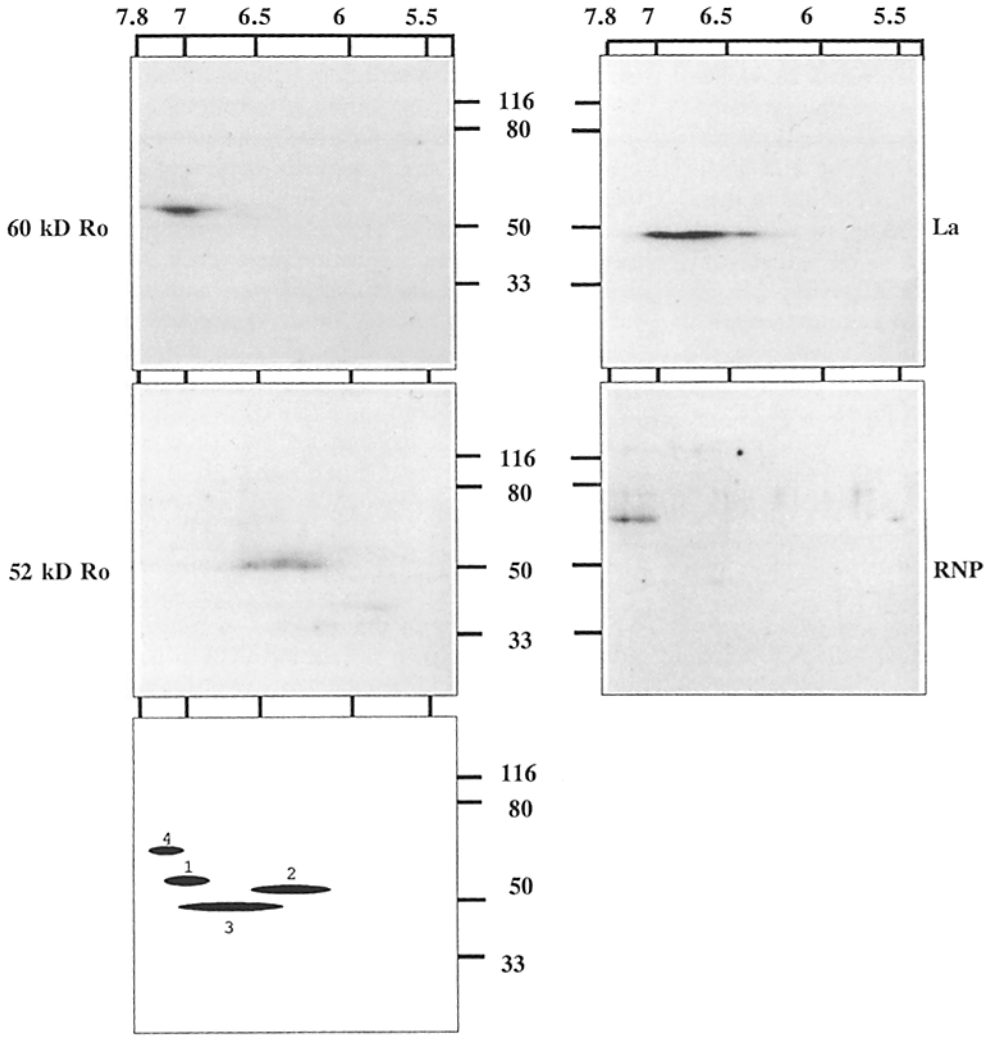

Figure 4. Two-dimensional immunoblots of keratinocyte lysates with autoantibodies. Keratinocyte lysates from unirradiated cells were subjected to isoelectric focusing in the first dimension, and gel electrophoresis on 15% SDS-PAGE in the second dimension. The proteins were then transferred to Immobilon® and blotted with a monospecific human serum to the 52-kD Ro protein, or with affinity-purified antibodies to the 60-kD Ro, 48-kD La, and 70-kD U1-RNP proteins. The positions of molecular weight standards are marked on the *y*-axis; the values on the *x*-axes represent the pI range (7.8–5.5). (*Bottom left*) Representation of the relative positions of the four antigens. Spots marked 1, 2, 3, and 4 represent the 60-kD Ro, 52-kD Ro, La, and U1-RNP, respectively. The U1-RNP data were obtained in a single experiment; all other two-dimensional blots were performed on at least two occasions.

to evaluate their distribution in apoptotic cells. In initial studies, 18 out of 21 sera positive for Ro by immunodiffusion showed intense staining of the RNA-containing surface blebs (data not shown). No staining of apoptotic surface structures was seen using eight different sera obtained from healthy adults (data not shown). For subsequent studies, we used a monospecific human serum to the 52-kD Ro protein, and affinity-purified antibodies to the 60-kD Ro, the 48-kD La, and the 70-kD U1-RNP proteins to examine the distribution of these antigens in apoptotic cells. Before use in immunofluorescence microscopy, these reagents were characterized by two-dimensional immunoblotting to confirm that they each recognized a single protein of the predicted size and charge (Fig. 4) (38). In each case, the immunodominant protein focused as a series of isoforms with estimated isoelectric points ranging from 7.0–7.5 (60-kD Ro), 6.2–6.7 (52-kD Ro), 6.5–7.2 (48-kD La), and 7.2–7.6 (70 kD U1-RNP).

When these reagents were used in immunofluorescence studies of unirradiated keratinocytes, antibodies to Ro stained the cytoplasm diffusely and stained the nucleus with a speckled pattern that excluded nucleoli (Fig. 5 *D*). A similar pattern was obtained with affinity-purified antibodies to La, although the cytoplasmic staining was less prominent (data not shown). PI, used without RNase, stained the nucleus, with prominent nucleoli, as well as the cytoplasm (Fig. 5 *E*). In apoptotic keratinocytes, the small surface blebs stained intensely with antibodies to Ro (Fig. 5, *A* and *G*) and with PI (Fig. 5 *B*), whereas the cytoplasmic staining of both was conspicuously decreased (Fig. 5, *A–C*, *G*). Ro staining was excluded from areas of condensed chromatin, but stained intensely

Figure 5. Autoantigens are found in blebs at the surface of apoptotic keratinocytes. (*A–F*). Irradiated (*A–C*) and unirradiated (*D–F*) keratinocytes were double stained with a monospecific human serum to 52-kD Ro (*A* and *D*) and with PI (*B* and *E*), and examined by confocal fluorescence microscopy. Ro antibodies were visualized with FITC-goat anti-human antibodies and assigned the color green, whereas PI staining was assigned as red. When green and red images were merged using confocal software, overlapping pixels appeared orange/yellow (*C* and *F*). In irradiated cells, 52-kD Ro (*A*) and PI (*B*) both stain the small surface blebs. Cytoplasmic staining of both is diminished when compared with controls (*D–F*). (*G–L*). Irradiated keratinocytes were double stained with PI and one of the following affinity purified antibodies: 60-kD Ro (*G*), La (*H* and *I*), and U1-RNP (*J*), or a mAb to TMG (*K* and *L*). Antibody- and PI-staining were captured separately as above, and images merged as in *A–F*. Only merged images are

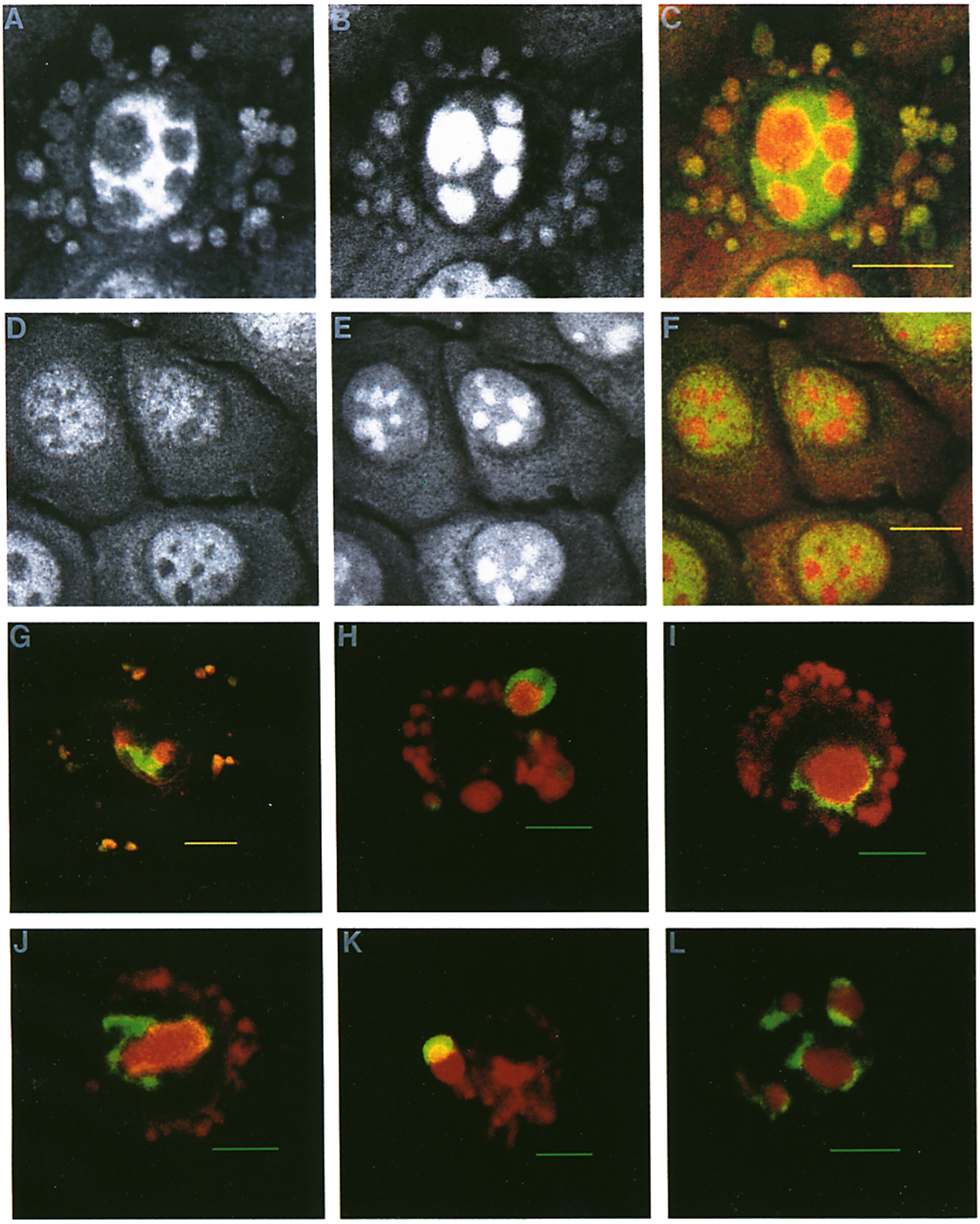

shown, with green staining representing antibody, red representing PI, and overlapping pixels appearing orange/yellow. 60-kD Ro is seen in surface blebs (*G*), in contrast to La (*H* and *I*), 70-kD U1-RNP (*J*), and TMG (*K* and *L*) which are excluded from these structures. (*H–K*) Distribution of these antigens in a rim around the condensed nucleus (*I* and *J*), fragmented nucleus (*L*), or apoptotic bodies (*H* and *K*). The data shown are representative of experiments that were performed on at least four separate occasions with each different antibody. Bars: (*A–G*) 10 μm; (*H–L*) 5 μm.

around these areas (Fig. 5 *A*). Where apoptotic bodies were seen at the cell surface, a characteristic rim of Ro staining could often be seen around a core of nucleic acid (data not shown). Neither La nor U1-RNP was detected in the small RNA-containing surface blebs (Fig. 5, *H–J*). Instead, their staining was exclusively nuclear in the early stages of apoptosis, and was visualized as a bright eccentric rim of ribonucleoproteins around a core of nucleic acid (Fig. 5, *I* and *J*). In the later stages of apoptosis, La and U1-RNP staining was detected at the cell surface surrounding large blebs containing nucleic acid (Fig. 5 *H*). The staining pattern obtained with antibodies to the 70-kD protein component of U1-RNP was confirmed and extended by staining apoptotic cells with mAbs to TMG (39). These antibodies recognize the unique 5′-modification of the small RNA components of the spliceosome, multiple components of which are targeted by the immune system in lupus. TMG did not stain the small surface blebs (Fig. 5 *K*), but stained as a bright rim around fragmented nuclear material, either still within the cell (Fig. 5 *L*), or at the surface (Fig. 5 *K*). Colocalization studies with DAPI or nick labeling confirmed that the La- and TMG-stained structures contained DNA in their core (data not shown).

Small Surface Blebs on Apoptotic Cells Contain Fragmented ER and Ribosomes. The enrichment of RNA in small surface blebs was accompanied by a marked decrease in its cytoplasmic staining (compare Fig. 5, *B* and *E*). This suggested that the blebs might contain ribosomes, as >70% of cytoplasmic RNA is comprised of ribosomal RNA. Furthermore, since the ER fragments and moves outwards early in apoptosis (9), we wondered whether the apically directed movement of RNA represented a membrane-based translocation. To address this, we used lectin staining (FITC-Con A) to probe for any glycoproteins within surface blebs. In apoptotic cells that were incubated with FITC-Con A before permeabilization with acetone and subsequent staining with PI, a thin rim of FITC-Con A was visible around, but not within, areas that stained strongly with PI (Fig. 6, *A* and *B*). This was consistent with lectin binding to plasma membrane glycoproteins. In apoptotic cells that were permeabilized before incubation with FITC-Con A, clear substructure within the blebs was evident (Fig. 6, *C* and *D*): blebs appeared to be composed of multiple small, round, vesicular structures, defined by FITC-Con A staining around a central unstained area. This heterogeneous staining within the blebs was similar

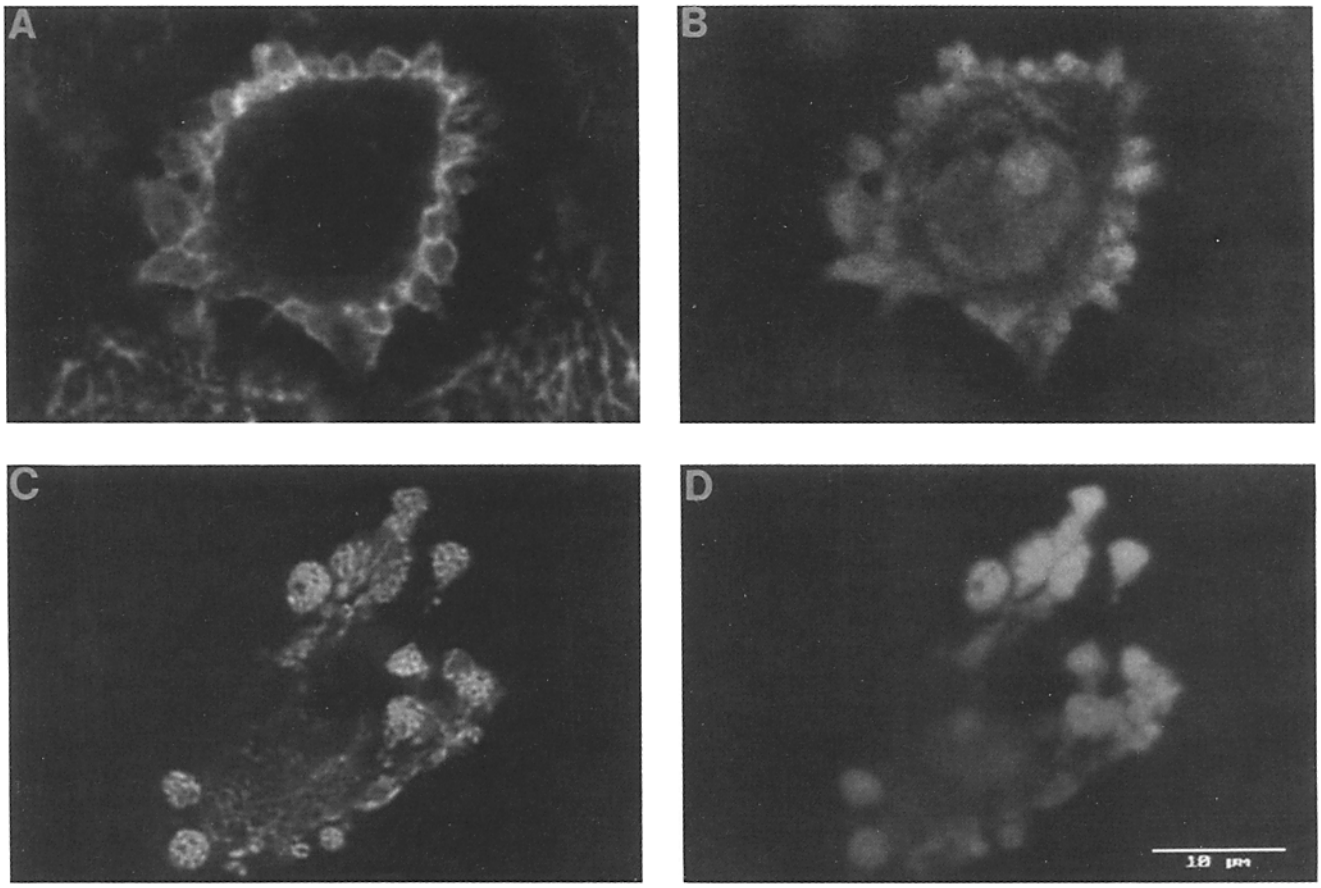

Figure 6. FITC-Con A staining of irradiated keratiocytes. (*A* and *B*) Irradiated keratinocytes were fixed and stained with FITC-Con A (*A*). They were subsequently permeabilized and stained with PI (*B*). Lectin-staining outlines the PI-containing surface blebs. (*C* and *D*). Irradiated keratinocytes were fixed and permeabilized before double staining with FITC-Con A (*C*) and PI (*D*). Lectin staining of both the surface and the interior of the blebs are seen. The internal staining is heterogeneous, and may outline vesicles. This experiment was repeated on three separate occasions with identical results. Bar, 10 μm.

to, but much better defined than the heterogeneity previously seen with PI or Ro (Fig. 3 *A* and Fig. 5, *A* and *B*).

We further investigated the contents of the small surface blebs by using mAbs to BiP (GRP78) (Fig. 7, *A* and *B*) or ribosomal protein S1 (Fig. 7, *C* and *D*) in immunofluorescence studies. Antibodies to BiP (40), a resident ER lumenal protein, stained strongly and specifically in unirradiated keratinocytes; staining was reticular in pattern, and was most intense in the perinuclear region (Fig. 7 *A*). In contrast, there was strong staining within the surface blebs of apoptotic cells, with diminished staining towards the perinuclear region (Fig. 7 *B*). Ribosomal protein S1 stained with a similar reticular pattern in unirradiated cells (Fig. 7 *C*), and also demonstrated prominent nucleolar staining as previously described (41). Apoptotic cells showed prominent staining within their surface blebs, with decreased staining towards the perinuclear region (Fig. 7 *D*). Isotype-matched, irrelevant mAbs did not stain the structures seen with the anti-BiP and anti-ribosomal S1 antibodies (data not shown).

To further resolve the internal structure of small surface blebs, irradiated keratinocytes were fixed in glutaraldehyde and processed for electron microscopy. Thin sections through the apical portion of irradiated cells were examined for surface blebs with a size of about 1.5 μm. Although such structures could be identified, the blebs appeared to contain a granular substance that could not be further resolved using this method of fixation. Since our confocal microscopy data had strongly suggested the presence of multiple small membrane-bound vesicular structures within the surface blebs (Fig. 6 *C*), we subsequently used a microwave fixation protocol that is reported to improve preservation of membranes, perhaps by optimizing osmication (42–44). Numerous surface blebs of the expected size were identified in apoptotic cells that had been fixed using this technique (Fig. 8 *A*). Consistent with our confocal studies, these structures were most prominent at the apical surface of irradiated keratinocytes. Thus, many sections that optimally demonstrated the surface blebs did not also traverse the nucleus (Fig. 8 *A*). However, other micrographs clearly showed both structures (Fig. 8 *B*), and confirmed the impression obtained from confocal microscopy that surface blebbing was prominent before nuclear changes of apoptosis became pronounced. The surface blebs were membrane bound, and uranyl acetate staining demonstrated the bilayer structure of the limiting membrane. Many sections showed the blebs either forming at the plasma membrane (Fig. 8, *B* and *C*), or cut in a plane that made

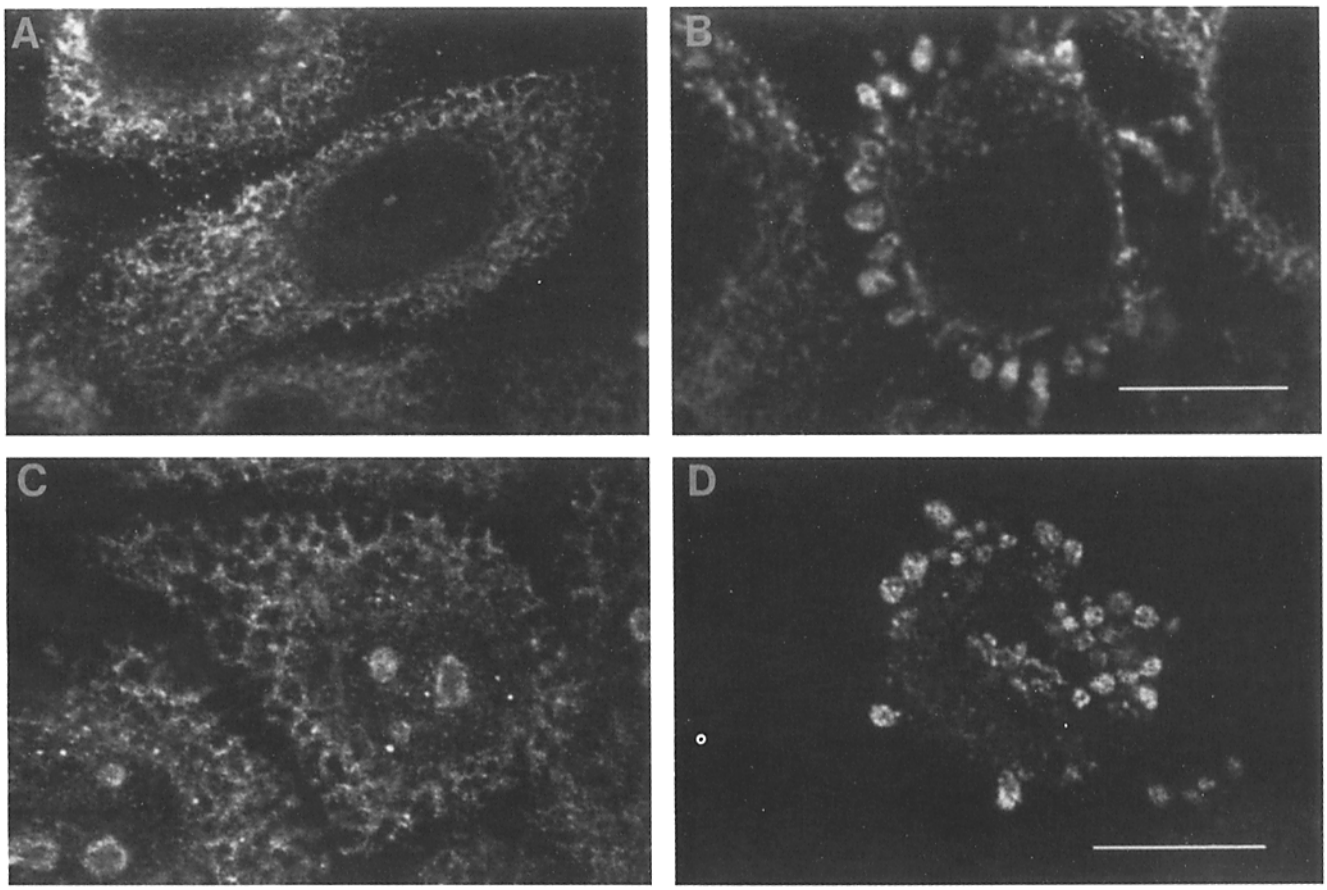

Figure 7. Staining of keratinocytes with antibodies to BiP (*A* and *B*) or antiribosomal protein S1 (*C* and *D*). Control (*A* and *C*) and irradiated (*B* and *D*) keratinocytes were stained with mAbs to BiP (*A* and *B*) or ribosomal protein S1 (*C* and *D*), and visualized by confocal fluorescence microscopy. The cells were fixed in methanol and acetone (41) before staining with antiribosomal S1. Identical results were obtained in two separate experiments performed with each antibody. Bar, 10 μm.

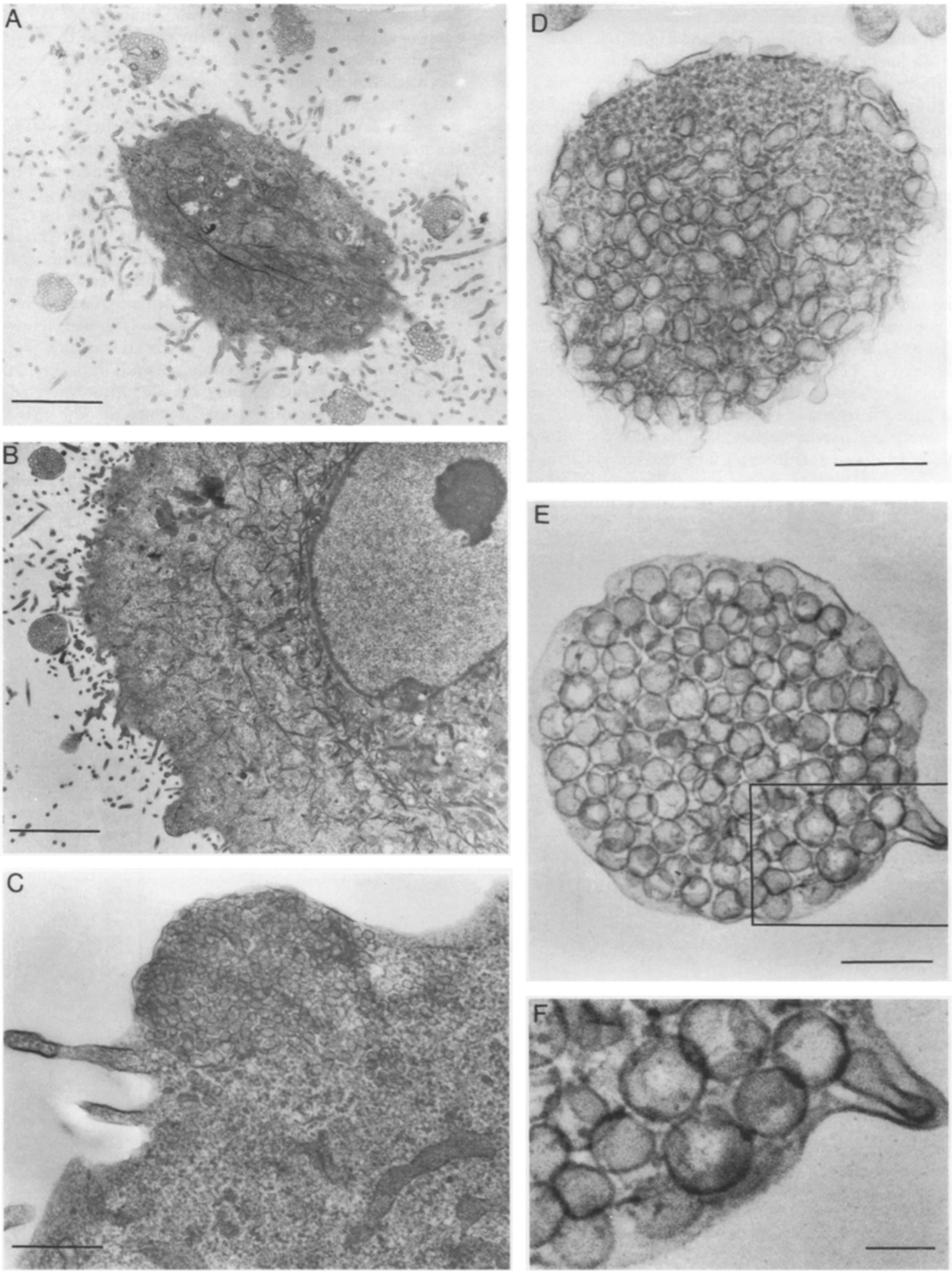
A
B
C
D
E
F

them appear separate from the cell body (Fig. 8, *A* and *B*). Most surface blebs were round, with a mean diameter of 1.3 ± 0.23 μm (mean ± SD, n = 70). The limiting plasma membrane of these blebs enclosed multiple round membrane-bound vesicles with a diameter of 100 ± 13.7 nm (mean ± SD, n = 267) (Fig. 8, *D* and *E*). The vesicles were clear, contained minimal ground substance, and were surrounded by a bilayer as confirmed by uranyl acetate staining (Fig. 8 *F*). Granular structures that appeared to be ribosomes were seen in many blebs (Fig. 8, *D* and *E*). In areas of the cell underlying blebs, rough ER could be seen just beneath the plasma membrane (Fig. 8 *C* and data not shown). Numerous bundles of cytokeratins were prominent in many sections (Fig. 8, *A* and *B*). When normal keratinocytes were microwave fixed and processed identically, very few surface blebs with internal vesicles could be found. The few that were present were smaller (<0.5 μm diameter) than in irradiated cells (data not shown).

Discussion

Autoantigens Are Clustered in the Surface Blebs of Apoptotic Cells. These studies have defined a population of RNA-containing blebs at the surface of apoptotic cells, that had previously been visualized by phase- and scanning electron-microscopy (37). Blebs are numerous, ~1.4 μm in diameter, and are restricted to the apical surface of apoptotic keratinocytes. Blebs are bounded by a membrane bilayer that is continuous with the plasma membrane, are filled with multiple membranous vesicles of uniform size (about 100 nm in diameter), and contain BiP (an ER lumenal marker), ribosomes, and the ribonucleoprotein autoantigen, Ro. Both Ro and ribosomes are prominent targets of the immune system in lupus, and it is particularly striking that other components of the ER have also been demonstrated to act as autoantigens in this disease. These include the lumenal ER protein, calreticulin (45), the signal recognition particle (46, 47), and acidic phospholipids (for a review see reference 3). These small surface blebs therefore constitute a novel cluster of autoantigens that appear to rise from rough ER, but have a surface, rather than an internal location.

Although Ro binds to a family of small cytoplasmic RNAs, it is not restricted to the cytoplasm (48), and is also found in the apoptotic nucleus. Much of this nuclear Ro is reorganized during apoptosis. Ro is excluded from the nucleoplasm as the chromatin becomes condensed, and becomes concentrated around the rim of apoptotic bodies after nuclear fragmentation. La and the snRNPs are similarly rearranged. After forming within the cell, the apoptotic bodies move to the surface where they give rise to a population of larger surface structures containing fragmented DNA. These apoptotic bodies also contain a distinct cluster of autoantigens that are targeted in patients with lupus, including nucleosomes (5, 6, 49), Ro (50), La (51), and snRNPs (52). We propose that the majority of recognized autoantigens in lupus are located within these two distinct types of surface structures.

The conspicuous movement of cytoplasmic Ro to small surface blebs early in apoptosis implies that cytoplasmic Ro has an affinity for the other components in these blebs, and suggests that Ro has a function that is performed at the site of ER–ribosome interaction. Such functions might include, but are not limited to, a role in protein synthesis, control of translation, and protein translocation into the ER. Indeed, such roles have previously been proposed (50, 53). Further study of the interaction of Ro with the various subcomponents of this particle may shed light on the function and interactions of Ro.

ER and Nuclear Membranes Are Sites of Free Radical Generation in Apoptotic Cells. After an apoptotic signal, cells sustain progressive lipid peroxidation, reflecting the generation within apoptotic cells of lipid-diffusible reactive oxygen species (21). In the ER, induction of lipid peroxidation results in membrane fragmentation into small vesicles (54), with some thickening of the bilayer (55). These vesicular fragments strongly resemble the 100-nm vesicles within membrane blebs (Fig. 8) that stain with specific ER lumenal markers (Fig. 7). It is therefore possible that these vesicles arise as a consequence of unopposed lipid peroxidation in the ER membranes of apoptotic cells. The presence of peroxidated lipids in the small vesicles remains to be directly demonstrated.

The major sites of free radical generation in cells include mitochondria, ER, and nuclear membranes (21, 56, 57). The free radicals produced at these sites are highly reactive species, and their damaging activities are focused at sites of their generation, where macromolecules may sustain oxidative damage (58). It is highly significant therefore that the two populations of autoantigens targeted in patients with lupus are topologically restricted to sites of free radical generation in apoptotic cells, that is, to areas of vesiculating ER (Ro, ribosomes, and ER proteins), and to the rim of apoptotic bodies that are surrounded by nuclear membrane (Ro, La, dsDNA, and snRNPs). It is also of interest that autoantibodies to mitochondrial components (e.g., cytochrome c) have been observed in patients with lupus and related diseases (59). A common feature of self-antigens at these sites might be their vulnerability to oxidative damage.

It has been proposed that some autoreactive T cells escape tolerance induction because they are directed against minor (cryptic) determinants on self-antigens that are not efficiently generated during antigen processing (60). These autoreactive cells may become pathogenic if that cryptic determinant is subsequently revealed (61–63). A number of free radical–induced modifications of proteins have been described that may reveal potentially cryptic determinants. These include fragmentation (64, 65), amino acid modifications (e.g., trypto-

Figure 8. Electron microscopy of irradiated keratinocytes. Irradiated keratinocytes were fixed in glutaraldehyde using microwave irradiation, and processed for electron microscopy. Surface blebs containing multiple vesicles are seen. Blebs are studded with numerous granular particles that appear to be ribosomes. (*F*) An enlargement of the boxed area shown (*E*) to highlight the bilayer nature of the membranes. Identical results were obtained in two separate experiments. Bars: (*A*) 2.9 μm; (*B*) 2 μm; (*C*) 0.5 μm; (*D*) 0.3 μm; (*E*) 0.25 μm; and (*F*) 0.1 μm.

phan loss) (64), and novel sensitivity to protease attack (66). Our recent identification of a specific cleavage of the 70-kD U1-RNP antigen in apoptotic cells (L. Casciola-Rosen, and A. Rosen, unpublished results) supports the hypothesis that site-specific modification of proteins may generate unique peptide fragments. The strong association of particular autoantibody responses with specific MHC class II molecules in patients with SLE may reflect the ability of these class II molecules to capture and present self-peptides to T cells (67, 68).

Apoptosis in Murine Models of Lupus. MRL mice spontaneously develop late onset autoimmune disease (69), and develop autoantibodies with a specificity very similar to that seen in human disease, including antibodies to dsDNA and Sm (70). When MRL mice are, in addition, homozygous for the lpr mutation, they develop massive lymphadenopathy, and have marked acceleration of autoimmune disease (69). The lpr mutation (71) results from integration of the retrotransposon, ETn into an intron in the *fas* gene, with diminished fas expression (72, 73) and fas-mediated apoptosis. The abnormality in apoptosis has been proposed to be responsible for defective negative selection of self-reactive T lymphocytes in the thymus (71). Apoptosis in the thymus is not only a mechanism for the deletion of self-reactive clones, but is also an abundant source of apoptotic autoantigens to which the organism must become tolerant. The failure of fas-mediated T cell apoptosis within the thymus of developing lpr/lpr mice may not only facilitate the persistence of autoreactive clones, but may also deprive the organism of the opportunity to generate a full repertoire of "apoptotic" autoantigens to which to become tolerant. The specificity of the immune response to a restricted, but common group of autoantigens in mouse and human disease is therefore particularly relevant.

Autoantigen Clusters in Lupus: A Model. In these studies, we have shown that apoptosis induces the physical clustering of autoantigens in two distinct populations of cell surface structures. As these blebs contain ER (small blebs) or nuclear membrane (apoptotic bodies), sites of unbuffered generation of reactive oxygen species in apoptotic cells, we propose that the contained autoantigens have in common a vulnerability to oxidative modification, targeted by metal binding or active sites (58, 66, 74). In a genetically susceptible individual, at high rates of generation of novel fragments (e.g., irradiation, heat shock, bacterial or viral infection, or xenobiotic exposure), the appropriate MHC class II molecules may capture and present self-peptides that were previously cryptic (62, 63, 75, 76). As in other systems, the immune response to this self-peptide may subsequently diversify to other areas on the self-molecule to which the organism was previously tolerant (60, 77). Subsequent reexposure of the primed immune system to even low levels of "apoptotic" autoantigens (e.g., sun exposure) may lead to the clinical flares in this disease. The revelation of previously cryptic peptides to the immune system by oxidative modification of proteins may also be applicable to other autoimmune diseases.

We thank Carolyn Machamer for critical review of the manuscript, Hugh Rosen for numerous thoughtful suggestions, Alan Aderem and Joe Ahearn for helpful discussions, Ed Cluett for suggesting the microwave fixation and help in its execution, and Mike Delannoy for his invaluable assistance with confocal and electron microscopy. We also thank the members of the Dermatoimmunology laboratory for help with keratinocyte cultures and screening of sera.

This work was supported in part by National Institutes of Health (NIH) grants AR-32490 and AR-40018 (G. Anhalt). A. Rosen was supported by the NIH Physician-Scientist Program, and by American Cancer Society Institutional Research Grant 11-33.

This paper is dedicated to the memory of Zanvil A. Cohn.

Address correspondence to Dr. A. Rosen, Department of Medicine, Johns Hopkins University School of Medicine, 720 Rutland Avenue, Baltimore, MD 21205.

Received for publication 10 December 1993.

References

1. Pistiner, M., D.J. Wallace, S. Nessim, A.L. Metzger, and J.R. Klinenberg. 1991. Lupus erythematosus in the 1980s: A survey of 570 patients. *Semin. Arthritis. Rheum.* 21:55.
2. Tan, E.M., E.K.L. Chan, K.F. Sullivan, and R.L. Rubin. 1988. Antinuclear antibodies (ANAs): diagnostically specific immune markers and clues toward the understanding of systemic autoimmunity. *Clin. Immunol. Immunopathol.* 47:121.
3. Harris, E.N. 1990. Antiphospholipid antibodies. *Br. J. Haematol.* 74:1.
4. Tan, E.M. 1991. Autoantibodies in pathology and cell biology. *Cell.* 67:841.
5. Mohan, C., S. Adams, V. Stanik, and S.K. Datta. 1993. Nucleosome: a major immunogen for pathogenic autoantibody-inducing T cells of lupus. *J. Exp. Med.* 177:1367.
6. Burlingame, R.W., R.L. Rubin, R.S. Balderas, and A.N. Theofilopoulos. 1993. Genesis and evolution of antichromatin autoantibodies in murine lupus implicates T-dependent immunization with self antigen. *J. Clin. Invest.* 91:1687.
7. Diamond, B., J.B. Katz, E. Paul, C. Aranow, D. Lustgarten, and M.D. Scharff. 1992. The role of somatic mutation in the pathogenic anti-DNA response. *Annu. Rev. Immunol.* 10:731.
8. Sano, H., and C. Morimoto. 1981. Isolation of DNA from

DNA/anti-DNA antibody immune complexes in systemic lupus erythematosus. *J. Immunol.* 126:538.
9. Wyllie, A.H., J.F.R. Kerr, and A.R. Currie. 1980. Cell death: the significance of apoptosis. *Int. Rev. Cytol.* 68:251.
10. Cohen, J.J., and R.C. Duke. 1992. Apoptosis and programmed cell death in immunity. *Annu. Rev. Immunol.* 10:267.
11. Ellis, R.E., J. Yuan, and H.R. Horvitz. 1991. Mechanisms and functions of cell death. *Annu. Rev. Cell Biol.* 7:663.
12. Vaux, D.L. 1993. Toward an understanding of the molecular mechanisms of physiological cell death. *Proc. Natl. Acad. Sci. USA.* 90:786.
13. Umansky, S.R., B.A. Korol, and P.A. Nelipovich. 1981. In vivo DNA degradation in thymocytes of γ-irradiated or hydrocortisone-treated rats. *Biochem. Biophys. Acta.* 655:9.
14. Gobe, G.C., R.A. Axelsen, B.V. Harmon, and D.J. Allan. 1988. Cell death by apoptosis following X-irradiation of the foetal and neonatal rat kidney. *Int. J. Radiat. Biol.* 54:567.
15. Raff, M.C. 1992. Social controls on cell survival and cell death. *Nature (Lond.).* 356:397.
16. Itoh, N., S. Yonehara, A. Ishii, M. Yonehara, S.-I. Mizushima, M. Sameshima, A. Hase, Y. Seto, and S. Nagata. 1991. The polypeptide encoded by the cDNA for human cell surface antigen Fas can mediate apoptosis. *Cell.* 66:233.
17. Rabizadeh, S., J. Oh, L.-t. Zhong, J. Yang, C.M. Bitler, L.L. Butcher, and D.E. Bredesen. 1993. Induction of apoptosis by the low-affinity NGF receptor. *Science (Wash. DC).* 261:345.
18. Mosser, D.D., and L.H. Martin. 1992. Induced thermotolerance to apoptosis in a human T lymphocyte cell line. *J. Cell. Physiol.* 151:561.
19. Zychlinsky, A., M. Prevost, and J. Sansonetti. 1992. *Shigella flexneri* induces apoptosis in infected macrophages. *Nature (Lond.).* 358:167.
20. Levine, B., Q. Huang, J.T. Isaacs, J.C. Reed, D.E. Griffin, and J.M. Hardwick. 1993. Conversion of lytic to persistent alphavirus infection by the bcl-2 cellular oncogene. *Nature (Lond.).* 361:739.
21. Hockenbery, D.M., Z.N. Oltvai, X.-M. Yin, C.L. Milliman, and S.J. Korsmeyer. 1993. Bcl-2 functions in an antioxidant pathway to prevent apoptosis. *Cell.* 75:241.
22. Oltvai, Z.N., C.L. Milliman, and S.J. Korsmeyer. 1993. Bcl-2 heterodimerizes in vivo with a conserved homolog, Bax, that accelerates programed cell death. *Cell.* 74:609.
23. Boise, L.H., M. Gonzalez-Garcia, C.E. Postema, L. Ding, T. Lindsten, L.A. Turka, X. Mao, G. Nunez, and C.B. Thompson. 1993. bcl-x, a bcl-2–related gene that functions as a dominant regulator of apoptotic cell death. *Cell.* 74:597.
24. Veis, D.J., C.M. Sorenson, J.R. Shutter, and S.J. Korsmeyer. 1993. Bcl-2–deficient mice demonstrate fulminant lymphoid apoptosis, polycystic kidneys, and hypopigmented hair. *Cell.* 75:229.
25. Furukawa, F., M. Kashihara-Sawami, M.B. Lyons, and D.A. Norris. 1990. Binding of antibodies to the extractable nuclear antigens of SS-A/Ro and SS-B/La is induced on the surface of human keratinocytes by ultraviolet light (UVL): implications for the pathogenesis of photosensitive cutaneous lupus. *J. Invest. Dermatol.* 94:77.
26. Golan, T.D., K.B. Elkon, A.E. Gharavi, and J.G. Krueger. 1992. Enhanced membrane binding of autoantibodies to cultured keratinocytes of systemic lupus erythematosus patients after ultraviolet B/ultraviolet A irradiation. *J. Clin. Invest.* 90:1067.
27. LeFeber, W.P., D.A. Norris, S.R. Ryan, J.C. Huff, L.A. Lee, M. Kubo, S.T. Boyce, B.L. Kotzin, and W.L. Weston. 1984. Ultraviolet light induces binding of antibodies to selected nuclear antigens on cultured human keratinocytes. *J. Clin. Invest.* 74:1545.
28. Young, A.R. 1987. The sunburn cell. *Photodermatology.* 127:134.
29. Gavrieli, Y., Y. Sherman, and S.A. Ben-Sasson. 1992. Identification of programmed cell death in situ via specific labeling of nuclear DNA fragmentation. *J. Cell Biol.* 119:493.
30. Login, G.R., and A.M. Dvorak. 1985. Microwave energy fixation for electron microscopy. *Am. J. Pathol.* 120:230.
31. Johnson, A.M. 1986. Immunoprecipitation in gels. *In* Manual of Clinical Laboratory Immunology. N.R. Rose, H. Friedman, and J.L. Fahey, editors. American Society for Microbiology, Washington, DC. 14–24.
32. Buyon, J.P., S.G. Slade, E.K.L. Chan, E.M. Tan, and R. Winchester. 1990. Effective separation of the 52kDa SS-a/Ro polypeptide from the 48kDa SS-B/La polypeptide by altering conditions of polyacrylamide gel electrophoresis. *J. Immunol. Methods.* 129:207.
33. Towbin, H., T. Staehelin, and J. Gordon. 1979. Electrophoretic transfer of proteins from polyacrylamide gels onto nitrocellulose sheets: procedure and some applications. *Proc. Natl. Acad. Sci. USA.* 76:4350.
34. Olmsted, J.B. 1981. Affinity purification of antibodies from diazotized paper blots of heterogeneous protein samples. *J. Biol. Chem.* 256:11955.
35. Earnshaw, W.C., and J.B. Rattner. 1991. The use of autoantibodies in the study of nuclear and chromosomal organization. *Methods Cell Biol.* 35:135.
36. Casciola-Rosen, L.A., and A.L. Hubbard. 1992. Lumenal labeling of rat hepatocyte early endosomes. *J. Biol. Chem.* 267: 8213.
37. Arends, M.J., and A.H. Wyllie. 1991. Apoptosis: mechanisms and roles in pathology. *Int. Rev. Exp. Pathol.* 32:223.
38. Elkon, K.B., and P.W. Jankowski. 1985. Fine specificities of autoantibodies directed against the Ro, La, Sm, RNP, and Jo-1 proteins defined by two-dimensional gel electrophoresis and immunoblotting. *J. Immunol.* 134:3819.
39. Krainer, A.R. 1988. Pre-mRNA splicing by complementation with purified U1, U2, U4/U6 and U5 SnRNPs. *Nucleic Acids Res.* 16:9415.
40. Huovila, A.-P., A.M. Eder, and S.D. Fuller. 1992. Hepatitis B surface antigen assembles in a post-ER pre-Golgi compartment. *J. Cell Biol.* 118:1305.
41. Hugle, B., R. Hazan, U. Scheer, and W. Franke. 1985. Localization of ribosomal protein S1 in the granular component of the interphase nucleolus and its distribution during mitosis. *J. Cell Biol.* 100:873.
42. Marti, R., P. Wild, E.M. Schraner, M. Mueller, and H. Moor. 1987. Parathyroid ultrastructure after aldehyde fixation, high pressure freezing, or microwave irradiation. *J. Histochem. Cyto chem.* 35:1415.
43. Login, G.R., W.B. Stavinoha, and A.M. Dvorak. 1986. Ultrafast microwave energy fixation for electron microscopy. *J. Histochem. Cytochem.* 34:381.
44. Hopwood, D., G. Coghill, J. Ramsay, G. Milne, and M. Kerr. 1984. Microwave fixation: its potential for routine techniques in histochemistry, immunohistochemistry and electron microscopy. *Histochem. J.* 16:1171.
45. McCauliffe, D.P., F.A. Lux, T.-S. Lieu, I. Sanz, J. Hanke, M.M. Newkirk, L.L. Bachinski, Y. Itoh, M.J. Siciliano, M. Reichlin, et al. 1990. Molecular cloning, expression, and chromosome 19 localization of a human Ro/SS-A autoantigen. *J. Clin. Invest.* 85:1379.
46. Kole, R., L.D. Fresco, J.D. Keene, P.L. Cohen, R.A. Eisen-

berg, and P.G. Andrews. 1985. Alu RNA–protein complexes formed in vitro react with a novel lupus autoantibody. *J. Biol. Chem.* 260:11781.
47. Reeves, W.H., S.K. Nigam, and G. Blobel. 1986. Human autoantibodies reactive with the signal-recognition particle. *Proc. Natl. Acad. Sci. USA.* 83:9507.
48. Ben-Chetrit, E., E.K.L. Chan, K.F. Sullivan, and E.M. Tan. 1988. A 52-kD protein is a novel component of the SS-A/Ro antigenic particle. *J. Exp. Med.* 167:1560.
49. Bell, D.A., B. Morrison, and P. VandenBygaart. 1990. Immunogenic DNA-related factors: nucleosomes spontaneously released from normal murine lymphoid cells stimulate proliferation and immunoglobulin synthesis of normal mouse lymphocytes. *J. Clin. Invest.* 85:1487.
50. Wolin, S.L., and J.A. Steitz. 1984. The Ro small cytoplasmic ribonucleoproteins: identification of the antigenic protein and its binding site on the Ro RNAs. *Proc. Natl. Acad. Sci. USA.* 81:1996.
51. Lerner, M.R., J.A. Boyle, J.A. Hardin, and J.A. Steitz. 1981. Two novel classes of small ribonucleoproteins detected by antibodies associated with lupus erythematosus. *Science (Wash. DC).* 211:400.
52. Lerner, M.R., and J.A. Steitz. 1979. Antibodies to small nuclear RNAs complexed with proteins are produced by patients with systemic lupus erythematosus. *Proc. Natl. Acad. Sci. USA.* 76:5495.
53. Bachmann, M., M.J. Mayet, H.C. Schroder, K. Pfeifer, K.-H. Meyer zum Buschenfelde, and W.E.G. Muller. 1987. Identification of the Ro and La antigens in the endoribonuclease VII-ribonucleoprotein complex. *Biochem. J.* 243:189.
54. Pasquali-Ronchetti, I., A. Bini, B. Botti, G. De Alojsio, C. Fornieri, and V. Vannini. 1980. Ultrastructural and biochemical changes induced by progressive lipid peroxidation on isolated microsomes and rat liver endoplasmic reticulum. *Lab. Invest.* 42:457.
55. Kagan, V.E. 1988. Molecular mechanisms of biomembrane damage caused by lipid peroxidation. *In* Lipid peroxidation in biomembranes. CRC Press, Boca Raton, FL. 55–118.
56. Boveris, A., and B. Chance. 1973. The mitochondrial generation of hydrogen peroxide: general properties and effect of hyperbaric oxygen. *Biochem. J.* 134:707.
57. Cross, A.R., and O.T.G. Jones. 1991. Enzymic mechanisms of superoxide production. *Biochim. Biophys. Acta.* 1057:281.
58. Halliwell, B., and J.M.C. Gutteridge. 1986. Oxygen free radicals and iron in relation to biology and medicine: some problems and concepts. *Arch. Biochem. Biophys.* 246:501.
59. Mamula, M.J., R. Jemmerson, and J.A. Hardin. 1990. The specificity of human anti-cytochrome c autoantibodies that arise in autoimmune disease. *J. Immunol.* 144:1835.
60. Sercarz, E.E., P.V. Lehmann, A. Ametani, G. Benichou, A. Miller, and K. Moudgil. 1993. Dominance and crypticity of T cell antigenic determinants. *Annu. Rev. Immunol.* 11:729.
61. Gammon, G., and E.E. Sercarz. 1989. How some T cells escape tolerance induction. *Nature (Lond.).* 342:183.
62. Mamula, M.J., R.-H. Lin, C.A. Janeway, Jr., and J.A. Hardin. 1992. Breaking T cell tolerance with foreign and self coimmunogens. A study of autoimmune B and T cell epitopes of cytochrome c. *J. Immunol.* 149:789.
63. Lipham, W.J., T.M. Redmond, H. Takahashi, J.A. Berzofsky, B. Wiggert, G.J. Chader, and I. Gery. 1991. Recognition of peptides that are immunogenic but cryptic: mechanisms that allow lymphocytes sensitized against cryptic peptides to initiate pathogenic autoimmune processes. *J. Immunol.* 146:3757.
64. Davies, K.J.A. 1987. Protein damage and degradation by oxygen radicals. I. General aspects. *J. Biol. Chem.* 262:9895.
65. Wolff, S.P., and R.T. Dean. 1986. Fragmentation of proteins by free radicals and its effect on their susceptibility to enzymic hydrolysis. *Biochem. J.* 234:399.
66. Levine, R.L., C.N. Oliver, R.M. Fulks, and E.R. Stadtman. 1981. Turnover of bacterial glutamine synthetase: oxidative inactivation precedes proteolysis. *Proc. Natl. Acad. Sci. USA.* 78:2120.
67. Reveille, J.D., M.J. MacLeod, K. Whittington, and F.C. Arnett. 1991. Specific amino acid residues in the second hypervariable region of HLA-DQA1 and DQB-1 chain genes promote the Ro (SS-A)/La (SS-B) autoantibody responses. *J. Immunol.* 146:3871.
68. Arnett, F.C., M.L. Olsen, K.L. Anderson, and J.D. Reveille. 1991. Molecular analysis of major histocompatibility complex alleles associated with the lupus anticoagulant. *J. Clin. Invest.* 87:1490.
69. Cohen, P.L., and R.A. Eisenberg. 1991. Lpr and gld: single gene models of systemic autoimmunity and lymphoproliferative disease. *Annu. Rev. Immunol.* 9:243.
70. Eisenberg, R.A., E.M. Tan, and F.J. Dixon. 1978. Presence of anti-Sm reactivity in autoimmune mouse strains. *J. Exp. Med.* 147:582.
71. Watanabe-Fukunaga, R., C.I. Brannan, N.G. Copeland, N.A. Jenkins, and S. Nagata. 1992. Lymphoproliferation disorder in mice explained by defects in Fas antigen that mediates apoptotsis. *Nature (Lond.).* 356:314.
72. Wu, J., T. Zhou, J. He, and J.D. Mountz. 1993. Autoimmune disease in mice due to integration of an endogenous retrovirus in an apoptosis gene. *J. Exp. Med.* 178:461.
73. Chu, J.-L., J. Drappa, A. Parnassa, and K.B. Elkon. 1993. The defect in *Fas* mRNA expression in MRL/*lpr* mice is associated with insertion of the retrotransposon, *ETn*. *J. Exp. Med.* 178: 723.
74. Fucci, L., C.N. Oliver, M.J. Coon, and E.R. Stadtman. 1983. Inactivation of key metabolic enzymes by mixed function oxidation reactions: possible implications in protein turnover and ageing. *Proc. Natl. Acad. Sci. USA.* 80:1521.
75. Lehmann, P.V., T. Forsthuber, A. Miller, and E.E. Sercarz. 1992. Spreading of T-cell autoimmunity to cryptic determinants of an autoantigen. *Nature (Lond.).* 358:155.
76. Lin, R.-H., M.J. Mamula, J.A. Hardin, and C.A. Janeway, Jr. 1991. Induction of autoreactive B cells allows priming of autoreactive T cells. *J. Exp. Med.* 173:1433.
77. Mamula, M.J. 1993. The inability to process a self-peptide allows autoreactive T cells to escape tolerance. *J. Exp. Med.* 177:567.